



THE UNIVERSITY *of* EDINBURGH

Edinburgh Research Explorer

The importance of laboratory water quality for studying initial bacterial adhesion during NF filtration processes

Citation for published version:

Semiao, AJC, Habimana, O, Cao, H, Heffernan, R, Safari, A & Casey, E 2013, 'The importance of laboratory water quality for studying initial bacterial adhesion during NF filtration processes', *Water Research*, vol. 47, no. 8, pp. 2909-2920. <https://doi.org/10.1016/j.watres.2013.03.020>

Digital Object Identifier (DOI):

[10.1016/j.watres.2013.03.020](https://doi.org/10.1016/j.watres.2013.03.020)

Link:

[Link to publication record in Edinburgh Research Explorer](#)

Document Version:

Early version, also known as pre-print

Published In:

Water Research

General rights

Copyright for the publications made accessible via the Edinburgh Research Explorer is retained by the author(s) and / or other copyright owners and it is a condition of accessing these publications that users recognise and abide by the legal requirements associated with these rights.

Take down policy

The University of Edinburgh has made every reasonable effort to ensure that Edinburgh Research Explorer content complies with UK legislation. If you believe that the public display of this file breaches copyright please contact openaccess@ed.ac.uk providing details, and we will remove access to the work immediately and investigate your claim.



The importance of laboratory water quality for studying initial bacterial
adhesion during NF/RO filtration processes

A.J.C. Semião[§], O. Habimana[§], H. Cao, R. Heffernan, A. Safari, E. Casey^{*}

*School of Chemical and Bioprocess Engineering, University College Dublin (UCD), Belfield, Dublin 4,
IRELAND*

[§]Both authors contributed equally to this work

^{*}Corresponding author. Mailing address: University College Dublin, School of Chemical and
Bioprocess Engineering, Belfield, Dublin 4, IRELAND. Phone: +353 1 716 1974. Email:
evin.casey@ucd.ie

Keywords: Compaction, water quality, cell adhesion, nanofiltration

20 Abstract

21 Biofouling of nanofiltration (NF) and reverse osmosis (RO) membranes for water treatment
22 has been the subject of increased research effort in recent years. A prerequisite for
23 undertaking fundamental experimental investigation on NF and RO processes is a procedure
24 called compaction. This involves an initial phase of clean water permeation at high pressures
25 until a stable permeate flux is reached. However water quality used during the compaction
26 process may vary from one laboratory to another. The aim of this study was to investigate
27 the impact of laboratory water quality during compaction of NF membranes. A second
28 objective was to investigate if the water quality used during compaction influences initial
29 bacterial adhesion.

30 Experiments were undertaken with NF270 membranes at 15 bar for permeate volumes of
31 0.5L, 2L, and 5L using MilliQ, deionized or tap water. Membrane autopsies were performed
32 at each permeation point for membrane surface characterisation by contact angle
33 measurements, profilometry, and scanning electron microscopy. The biological content of
34 compacted membranes was assessed by direct epi-fluorescence observation following
35 nucleic acid staining. The compacted membranes were also employed as substrata for
36 monitoring the initial adhesion of *Ps. fluorescens* under dynamic flow conditions for 30
37 minutes at 5 minutes intervals.

38 Compared to MilliQ water, membrane compaction using deionized and tap water led to
39 decreases in permeate flux, increases in surface hydrophobicity and led to significant build-
40 up of a homogenous fouling layer composed of both living and dead organisms ($>10^6$
41 cells.cm⁻²). Subsequent measurements of bacterial adhesion resulted in cell loadings of
42 0.2×10^5 , 1.0×10^5 cells×cm⁻² and 2.6×10^5 cells.cm⁻² for deionized, tap water and MilliQ water

respectively. These differences in initial cell adhesion rates demonstrate that choice of laboratory water can significantly impact the results of bacterial adhesion on NF membranes. Standardized protocols are therefore needed for the fundamental studies of bacterial adhesion and biofouling formation on NF and RO membrane. This can be implemented by first employing pure water during all membrane compaction procedures and for the modelled feed solutions used in the experiment

1 Introduction

Nanofiltration (NF) and reverse osmosis (RO) membranes are commonly used for the removal of organic matter and trace contaminants, such as pesticides, during water treatment processes (Cyna et al. 2002). The efficiency of NF and RO processes is however adversely affected by membrane biofouling (Flemming 1997, Ivnitsky et al. 2007), principally due to the formation of biofilms (Flemming 2002). These ecosystems are usually made up of a community of dead and living microorganisms held together by a matrix of polysaccharides, lipids, proteins, organic matter, amongst other components (Flemming 2002). Biofilms are ubiquitous in NF and RO membrane plants (Houari et al. 2009, Vrouwenvelder et al. 1998, Vrouwenvelder et al. 2008, Khan et al. 2013) and are the Achilles heel of NF and RO processes (Flemming et al. 1997) as they are difficult to remove (Hijnen et al. 2012). Biofouling increases pressure drop along the membrane module (Vrouwenvelder et al. 2009a, Hijnen et al. 2009), leading to increased costs associated with energy consumption. The presence of biofilms on the membrane surface has also been shown to significantly affect permeate flux, and solute retention (Ivnitsky et al. 2005, Huertas et al.

2008). The decrease in solute retention and permeate flux has been attributed to enhanced concentration polarisation caused by the biofilms (Herzberg and Elimelech 2007). It has been shown that the concentration polarization also maintains the presence of biofilms by concentrating nutrients from the bulk environment (Chong et al. 2008, Vrouwenvelder et al. 2009b).

Biofilm formation is initiated by the irreversible adhesion of bacterial cells onto the membrane's surface, which is influenced by a number of factors. Firstly, the cell properties such as hydrophobicity (Ridgway et al. 1985) and cell surface charge (Subramani and Hoek 2008) have been found to affect adhesion. Secondly, the membrane physicochemical properties (roughness, charge and hydrophobicity) have been shown to impact the degree of adhesion. In general, the rougher and the more hydrophobic the membrane is, the more cells will adhere to the surface (Subramani and Hoek 2008, Myint et al. 2010, Khan et al. 2011). Finally, the presence of a conditioning layer on the membrane also affects bacterial adhesion (Subramani et al. 2009). A recent study has shown that a conditioning layer of salts and organic carbon promoted a homogeneous biofilm, whilst the absence of a conditioning layer resulted in a scattered and thin biofilm (Baek et al. 2011).

The intractable nature of the biofouling problem has led to a significant increase in research in this area in recent years (Herzberg and Elimelech 2007, Chong et al. 2008, Subramani and Hoek 2008, Baek et al. 2011, Fonseca et al. 2007). These studies range from the effects of biofilms on process performance (Ivnitsky et al. 2005, Huertas et al. 2008) to biofouling control through the design of antifouling membranes (Miller et al. 2012, Bernstein et al. 2011).

Although membrane biofouling research methodologies differ from one research laboratory to another, they generally share a common pre-treatment procedure involving the

compaction of the studied membrane prior to biofouling experiments. To accurately monitor flux changes and solute retention during NF and RO experiments caused by osmotic pressure or membrane fouling, membranes are purposely compacted to prevent changes due to the effect of pressure during the experiment. The compaction of NF and RO membranes is carried out under different filtration conditions depending on the laboratory they are carried out. The compaction is typically undertaken at a pressure between 6 and 25 bar and up to 18 hours in duration (Herzberg and Elimelech 2007, Baek et al. 2011, Fonseca et al. 2007, Suwarno et al. 2012). This translates into a typical water permeation volume between 2 L (membrane flux=50 L.h⁻¹.m⁻², time=18 hours and 22.44 cm² 100 membrane area) and 15 L (membrane flux=65 L.h⁻¹.m⁻², time=12 hours and 186 cm² 101 of membrane area) (Baek et al. 2011, Suwarno et al. 2012) calculated as: $V(L) = \text{Flux}(L/h.m^2) \times \text{time}(h) \times \text{Membrane Area}(m^2)$.

Although membrane compaction is a prerequisite to most NF and RO experimental studies, including bioadhesion/biofouling, the type of water used to compact the membrane may vary considerably from one laboratory to another. The water used in recent published studies on initial adhesion and biofouling experiments spans from non-sterilised tap water (Hijnen et al. 2009, Khan et al. 2011, Vrouwenvelder et al. 2009c, Vrouwenvelder et al. 2007, Botton et al. 2012, Khan et al. 2010), DI water (Huertas et al. 2008, Herzberg and Elimelech 2007, Myint et al. 2010, Baek et al. 2011, Lee et al. 2010) and MilliQ water (Chong et al. 2008, 2007, Pang et al. 2005). Tap water and DI water will vary in quality depending on the water source and the yearly season (Gibbs et al. 1993). In essence, the total carbon, biological and endotoxin contents will differ from one water type to another, whether the water is sterilized or not. Moreover, when considering filtration aspects, all insoluble water constituents will most certainly be deposited on the membrane surface during the

compaction, thus altering the membrane surface from its original state. The conditioning layer formed during the compaction pre-treatment of NF/RO is likely to result in altered surface characteristics thereby affecting subsequent biofouling experiments.

The objective of this study was to first demonstrate the impact of the choice of water used during compaction of NF membranes in terms of membrane performance, surface characterisation and secondly, to investigate whether the water used during membrane compaction also affects bioadhesion outcomes.

2 Materials and Method

2.1 Water source and characterisation

Three different water grades were used in our study: tap water provided by south Dublin water municipality, deionized water obtained by a purifying water system (Elgastat B124, Veolia, Ireland) and Grade 1 pure water ($18.2 \text{ M}\Omega\cdot\text{cm}^{-1}$) obtained by an Elga Process Water System (Biopure 15 and Purelab flex 2, Veolia, Ireland), hereafter referred to as MilliQ water. Conductivity and pH measurements were performed on all water samples at room temperature (20°C) and total organic carbon of all water samples was determined using a total organic carbon analyser (TOC-VCSH, Shimadzu, Ireland) in the NPOC mode, equipped with an automatic sample injector and an NDIR detector. Calibration standards were made using potassium hydrogen phthalate at different concentrations between 0 and 10 mgC/L. The water samples were collected in new 50 mL sterile Eppendorf tubes, filtered twice with

polyethersulphone 0.2 μm filters (Corning Incorporated, VWR Ireland), put in TOC vials that had been soaked overnight in 0.5 M NaOH in MilliQ water and left to dry at 30°C upside down to avoid any contamination from the air followed by a thorough rinsing with MilliQ water and analysed straight away. Measurement results are presented in Table 1. The measurements were carried out from samples taken between October and November 2012. In the particular case of MilliQ water, the samples have a measured TOC concentration that varied from 0.00 to 0.24 mgC.L^{-1} . The average value measured for 10 samples were $0.13 \pm 0.06 \text{ mgC.L}^{-1}$ (Table 1).

The total solids were measured by filling a glass vial with 40 mL of each water source and allowing it to evaporate in an oven at 100°C. The vial weight was measured before and after evaporation and the difference obtained in weight corresponded to the total solids weight. A control sample was used, where an empty vial was placed in the oven to ensure no floating particles present could affect the results.

The pH was measured with a HI1332 pH probe (Hannah, VWR, Ireland) and the conductivity was measured with a TetraCon 325 conductivity probe (WTW, VWR, Ireland).

The total amount of cells in each water source was determined as follows: a volume of 100 mL of MilliQ and tap water and 80 mL of DI water were filtered with a 0.2 μm filter (GTBP-25mm, Millipore, Ireland). The filter was then removed, placed in 3 mL of raw water without carbon (as explained in section 2.3.1) and stained with SYTO® 9 and PI dyes. The filter was then observed under an Epi-fluorescence microscope (Olympus BX 51) using a 40x objective. Fluorescent organisms were observed using two filter cubes each exciting SYTO® 9 and PI dyes at 450 nm and 550 nm respectively. At least ten micrographs were obtained at 5

random points on each compacted stained membrane sample. The number of fluorescent organism were then counted using Image J® (NIH, Bethesda, MD, USA).

2.2 Compaction experiment

NF 270 membranes (Filmtec Corp. USA) were used as the reference nanofiltration membrane in this study. The membranes were gently washed and left soaking overnight in the fridge in the water source they were going to be exposed to during the experiment in order to remove all the preservatives. The membrane compaction experiments were performed in Membrane Fouling Simulators (Vrouwenvelder et al. (2006)) at 15 bar pressure and a feed flow rate of 0.66L/min in each cell using one type of water grade for each experimental run. This flow rate corresponds to a velocity of 0.35 m/s, a Re_{dh} of 579 and a shear rate of 2588 s^{-1} in each cell.

The cross-flow system was equipped with a 10 L autoclavable feed tank (Nalgene, VWR Ireland) and a high pressure pump (P200 from Hydra-Cell, UK). The system was connected to three MFS devices placed in parallel holding each NF 270 membranes on the experimental rig at the start of compaction. The MFS cells are of the slit type channel height of 0.8 mm, width of 40 mm and length of 255 mm. Each membrane cell holds a membrane of 102 cm^2 . Separate experiments were carried out in the cross-flow system in order to confirm that the feed flow rate was distributed evenly by the three cells. The pressure on the outlet side of the slit feed channel of each of the 3 membrane cells was measured during operation at different flow rates and pressures. The pressure between the different MFS cells did not vary by more than 2% for the conditions tested, showing that the flow rate distributes

evenly in the system. Temperature was monitored in the feed tank with a temperature indicator (Pt 100, Radionics, Ireland) and maintained at $20^{\circ}\text{C} \pm 1^{\circ}\text{C}$ with a coil inside the tank connected to a temperature controlled MultiTemp III water bath (Pharmacia Biotech, Ireland). A back pressure regulator (KPB1L0A415P20000, Swagelok, UK) allows the pressurization of the system. The pressure was monitored in both feed and retentate side of the membrane cells with two pressure transducers (PTX 7500, Druck, Radionics, Ireland). The feed flow was measured using a flow meter (OG2, Nixon Flowmeters, UK). Datalogging was set-up for monitoring inlet and outlet pressure, feed flow rate and temperature (PicoLog 1000, PicoTechnology, Radionics, Ireland). The permeate volume collected was measured using 1000 mL graduated bottle, where the permeate volume was not returned to the feed tank. The permeate flux was determined by measuring a volume of permeate with a balance HCB123 balance (Adams, Astech Ireland) with a stopper. The P&ID of the crossflow filtration system is depicted in Figure 1.

Permeate flux and permeate conductivity measurements were performed throughout the compaction experiment. Once permeate levels reached 0.5L for each MFS device, the compaction was temporarily stopped to allow removal of one MFS device from the rig. Compaction was thereafter continued for the two remaining MFS devices until permeate levels reached 2L levels each, at which point the second MFS was removed from the system. The last MFS was left compacting until 5L permeate was collected.

Once removed from the rig system, the MFS device containing a compacted NF270 membrane was opened while submerged under the corresponding water type. Membrane

samples were immediately cut to size for autopsy and dynamic adhesion experiments as described in sections 2.2.1.4 and 2.3.2. The remainder of the membrane was left to dry in a closed box at room temperature for at least 48 hours to ensure the membrane was dry.

2.2.1 Surface characterisation assays of compacted NF270 membranes.

2.2.1.1 Profilometry

Optical profilometry analysis was carried out to examine the morphology and to quantify surface roughness. These measurements were carried out using a Wyko NT1100 optical profilometer operating in vertical scanning interferometry (VSI) mode. The R_q (root mean square roughness) was obtained on three different locations on each sample surface and an average value obtained.

2.2.1.2 Contact angle measurements

The Lifshitz-van der Waals (γ^{LW}), electron-donor (γ^-) and electron-acceptor (γ^+) surface tension components of dehydrated compacted NF 270 membrane samples (S) were determined by measuring contact angles using the following expression:

$$\cos\theta = -1 + 2 (\gamma_S^{LW} \gamma_L^{LW})^{\frac{1}{2}} / \gamma_L + 2 (\gamma_S^+ \gamma_L^-)^{\frac{1}{2}} / \gamma_L + 2 (\gamma_S^- \gamma_L^+)^{\frac{1}{2}} / \gamma_L \quad (1)$$

Contact angles (θ) and surface energy measurements (γ^S) of dehydrated compacted NF 270 membrane were measured at room temperature using a goniometer (OCA 20 from Dataphysics Instruments) with three static pure liquids (L): deionised water, diiodomethane and ethylene glycol.

221 The Lewis acid-base component was deduced from:

$$222 \quad \gamma_S^{AB} = 2\sqrt{(\gamma_S^+ \gamma_S^-)} \quad (2)$$

223 And the total surface energy was defined by:

$$224 \quad \gamma_S = \gamma^{AB} + \gamma^{LW} \quad (3)$$

225

226 Contact angle values and determined surface energies values presented in table 2
227 represent the mean of at least 10 measurements per compacted sample membrane.

228 Contact angle measurements were repeated in two independent replicates.

229

230 **2.2.1.3 Scanning electron microscopy**

231 For high resolution *ex-situ* observations of the membrane surface, the compacted NF 270
232 membranes were dehydrated by drying in air and then gold coated for 30 sec at x V 30 mA.

233 High magnification imaging of the membrane surfaces was performed under a Hitachi SEM
234 at the UCD Nano-imaging and Materials Analysis Centre.

235

236 **2.2.1.4 Biological assessment of NF 270 compacted membranes**

237 For assessing the biological presence on membranes samples, three regions of the
238 compacted NF 270 membranes were cut and placed in small petri dishes containing 3mL of
239 the water grade used during compaction. Membrane samples were then stained by adding
240 0.5 µL of 3.34mM SYTO® 9 green-fluorescent nucleic acid staining solution and 0.5 µL of 20
241 mM propidium iodide red-fluorescent nucleic stain. Stained membrane samples were

subsequently incubated in the dark for at least 15 minutes, after which the staining mix was discarded from the petri dish and a cover slip placed on membrane surfaces. The stained sample was then observed under an Epi-fluorescence microscope (Olympus Bx 51) using a 20x objective. Fluorescent organisms were observed using two filter cubes each exciting SYTO® 9 and PI dyes at 450nm and 550nm respectively. Ten micrographs were obtained at 5 random points on each compacted stained membrane sample. The number of fluorescent organism was then counted using Image J®, an image quantification software.

2.3 Initial adhesion assay on NF270 compacted membranes

2.3.1 Microbial strain and culture conditions

The *Pseudomonas fluorescens* NCTC 10038 was selected for dynamic adhesion assays on compacted NF 270 membrane. The cells were stored at -20°C with 20% volume glycerine as a cryoprotectant. Prior to experiments, cells were spread on King B agar (Oxoid) and incubated at 30°C overnight. Single colonies were then inoculated in were then cultured at 30°C and 150 rpm in Raw Water (RW) medium (tryptic soy broth 0.3 g.L⁻¹, sodium citrate Na₃C₆H₅O₇ 0.26 g.L⁻¹, NaHCO₃ 0.042 g.L⁻¹, NaCl 0.12 g.L⁻¹, KH₂PO₄ 0.063 g.L⁻¹, MgSO₄ 0.15 g.L⁻¹, NH₄Cl 0.005 g.L⁻¹, CaCl₂ 0.076 g.L⁻¹). When cell density reached 0.270 at OD₆₀₀, 12mL of the overnight culture were centrifuged at 7000 rpm for 10 minutes, before discarding supernatant. The remaining pellet was suspended with Raw Water medium containing no C-source (RW^{-C}) to a final volume of 1 mL. The cells were then stained by adding 0.5 µL of 3.34mM SYTO® 9 and 0.5 µL of 20 mM propidium iodide, followed by a 15 minutes incubation period at room temperature in the dark. The stained *Ps. fluorescens* cells were then centrifuged at 7000 rpm for 10 min before discarding the supernatant. The remaining

pellet was then re-suspended in 24 mL RW^{-c} medium prior to adhesion experiments order to attain a final cell concentration of 10⁷ cells.mL⁻¹.

2.3.2 Initial adhesion assay

Initial adhesion assays were performed on freshly cut compacted membranes that were placed on a support inserted in a flow cell (Model BST FC 81, Biosurface Technologies Corporation, Bozeman, MT) with modified channel dimensions of 0.8 by 12.7 by 47.5 mm. Compacted membranes were immobilized on the support using double sided tape, and hydration was ensured by filling the flow cell chamber with RW^{-c} prior to adhesion experiments. The flow cells are small continuous-flow systems with a glass viewing port that allowed *in situ* observation using an Epi-fluorescence microscope (Olympus BX 51) and a 20x objective. After removing bubbles from the system, “zero point” images of the NF270 compacted surface were recorded using two filters with excitation wavelengths set at λ_{ex} 450nm and λ_{ex} 550nm respectively. The freshly stained 24 mL *Ps. fluorescens* cells suspension was then circulated in the system at a volumetric flow rate of 1.5 ml min⁻¹. Adhesion time was recorded after 1, 5, 10, 15, 20, 25 and 30 minutes after the first observed cell adhered on the surface. Two images were recorded at λ_{ex} 450 nm and λ_{ex} 550 nm for each time point. Images of a size of 223 μ m x 1627 μ m were taken and analysed by counting adhered stained *Ps. fluorescens* cells using Image J®.

The initial adhesion kinetics of *Ps. fluorescens* on compacted membranes was established for all water sources using the following equation:

$$q(t) = q_{max} \cdot (1 - e^{-\beta t}) \quad (4)$$

where $q(t)$ is the bacterial loading as a function of time (t), the maximum cell loading q_{max} and the accumulation factor β obtained by the exponential fit of the adhesion experimental data. The linear region of the obtained curve was used to calculate the rate of adhesion by using the following expression:

$$k_d = \frac{\theta(t)}{\Delta t} \cdot \frac{1}{C_0} \quad (5)$$

where, k_d is the deposition rate of *Ps. fluorescens* on NF 270 membranes, $\vartheta(t)$ the number of adhered cells over a time period (Δt) between two time points and C_0 the initial bacterial suspension feed concentration.

3 Results

3.1 Water quality assessment

The different water qualities used for compacting NF 270 membranes used in this study were characterized prior to pre-compaction experiments and are presented in Table 1.

No detectable solids were measured in MilliQ and deionized water samples used in this study. MilliQ water had the lowest pH, total organic carbon, and conductivity values compared to deionized and tap water, respectively. MilliQ water has a very low conductivity

of $0.4 \mu\text{S.cm}^{-1}$ followed by DI water with a conductivity of $4 \mu\text{S.cm}^{-1}$. The highest conductivity obtained was for tap water with $168 \mu\text{S.cm}^{-1}$.

No cultivable cells (determined by CFU) were found in MilliQ. However deionized water was found to contain 170 times the number of cultivable organisms found in tap water. Direct count analysis (counting both culturable and non-culturable cells) revealed the presence of significant higher amounts of microorganisms in all tested water samples. Deionized water was found to contain 1800 and 15 times more microorganisms than in MilliQ and tap water, respectively. Moreover, deionized water also contained 850 and 30 times the amounts of dead/injured microorganisms found in MilliQ and tap water, respectively.

3.2 Effects of different water grades on NF 270 membrane performance during compaction.

In order to determine how each water source impacted the permeate flux during compaction, the permeate flux was measured for 0.5, 2 and 5 L of permeated water in the MFS cells. The results are presented in Figure 2. After a volume of 0.5 L of water permeated through the membrane, membranes compacted with tap water showed the lowest permeate flux of $195 \text{ L.h}^{-1}.\text{m}^{-2}.\text{bar}^{-1}$ compared to membranes compacted with deionized and MilliQ water, which had permeate fluxes of 283 and $339 \text{ L.h}^{-1}.\text{m}^{-2}.\text{bar}^{-1}$ respectively. Additionally, the use of tap water during compaction led to a constant decrease in permeate flux from $195 \text{ L.h}^{-1}.\text{m}^{-2}.\text{bar}^{-1}$ to $96 \text{ L.h}^{-1}.\text{m}^{-2}.\text{bar}^{-1}$ with the NF 270 membrane, as permeate volume increased from 0.5 L to 5 L. Visual inspection showed that the membrane surface was light coloured at 0.5 L and gradually increased to a dark yellow colour at 5 L (not shown) for tap water. In contrast, permeate flux stabilized after 0.5 L of water permeated through

the membrane for membranes compacted with deionized and MilliQ: from 2 L to 5 L the permeate flux stabilised at 251 and 301 L.h⁻¹.m⁻².bar⁻¹, respectively.

3.3. Effect of different water grades on NF 270 membrane surface properties.

The physico-chemical properties of NF 270 compacted membranes were evaluated by contact angle measurements and the associated van der Waals (γ^{LW}), Lewis Base (γ^-) and Lewis Acid (γ^+) components are presented in Table 2. Membranes exhibited increased hydrophobic character with increased permeate volumes. Membranes compacted with 5 L of MilliQ water showed the lowest hydrophobic properties ($\sigma_{water} = 49.7$), followed by membranes compacted with tap water ($\sigma_{water} = 56$), and deionized water ($\sigma_{water} = 68.9$) respectively, with the surface hydrophobicity varying in the following order: MilliQ < tap < DI water. Increasing permeate volumes can be seen to have not affected the van der Waals (γ^{LW}) character of the compacted membranes. However, membranes compacted with deionized water showed lowest van der Waal surface properties with 37 mJ.m⁻² compared to membranes compacted with MilliQ (42.3 mJ.m⁻²) and tap (45.5 mJ.m⁻²) water respectively. A significant decrease in Lewis Base (γ^-) membrane character was noticeable from 2L to 5L permeation using MilliQ water, whereas the same drop in Lewis base properties occurred earlier from 0.5L to 2L in membranes compacted with deionized and tap water. Membrane Lewis Acid (γ^+) character decreased by 2.5 fold from 0.5L and 2L permeated volumes of MilliQ, and during 2L to 5 L permeated volumes of deionized water. A 13.7 fold increase of Lewis Acid (γ^+) character was observed in compacted membrane after permeation of 2L to 5L tap water.

Roughness measurements of the different compacted membranes measured by optical profilometry are also presented in Table 2. No significant differences in surface roughness were observed for compacted membranes after permeation of 0.5L and 2L MilliQ, deionized water, and tap water. Although no differences in surface roughness were observed for membranes compacted with MilliQ (511 ± 143 nm) and deionized water (562 ± 123 nm) after 5 L permeation, membranes compacted with tap water showed highest roughness with 1166 ± 147 nm. Height topography results presented in Figure 3 showed that the surface of compacted membranes using MilliQ water (Figure 3 A) showed areas of very smooth surface topology profiles and areas with irregular and heterogeneous surface topology profiles, due to what looked like surface defects, presumably from the manufacturing process. Topological profiles of membranes compacted with deionized (Figure 3 C) and tap water (Figure 3 D) had a consistent and homogeneous roughness and no surface defects were observed. The surface of NF270 membranes compacted with tap water (Figure 3 D) had however frequent high narrow peaks compared to the smaller peaks obtained with the DI water compaction.

Closer examination of the membrane surfaces using scanning electron microscopy revealed distinct levels of deposition depending on water grade (Figure 4). The virgin NF270 surface was relatively smooth with the presence of numerous large heterogeneities (Figure 4 A). These structures were still visible after compaction with MilliQ water (Figure 4 B). Following compaction with deionized, the membrane's surface was covered by what seemed to be a matrix layer composed of microorganisms, and biological debris and possibly organic carbon (Figure 4 C). When compacted with the DI water the large heterogeneities found on the virgin membrane were not present, and the fouling layer caused by the DI water filtration,

although rough in the nanoscale, was homogeneous in the microscale. In this case a distinction needs to be made: although Table 2 shows similar roughness values (R_q) for the membranes compacted with the MilliQ water and the DI water, in the first case the membrane is very smooth with a scattered distribution of imperfections generally with valley widths between 20 to 50 μm (Figure 3 A) and in the second case, although the membrane is rough, it is homogeneously rough (Figure 3 B).

Membrane compaction using tap water led significant membrane fouling also including the presence of aquatic organisms such as diatoms, small microorganisms and a pronounced amount of debris (*e.g.* organic carbon) (Figure 4 D). The level of membrane fouling is apparent the degree of crack artefacts observed on the membrane's surface (Figure 4 C-D) caused by dehydration, especially in the case of samples compacted with tap water.

3.3 Biological assessment of NF 270 membranes after compaction using different water grades.

The biological characteristics of the compacted NF 270 membranes was assessed by nucleic acid BakLight® staining and is presented in Figure 5. Compaction using deionized and tap water led to a pronounced two log difference in the total presence of microorganisms (10^7 cells. cm^{-2}) on the membrane compared to membranes compacted with MilliQ water after 5L volume permeation (10^5 cells. cm^{-2}). A one log biological accumulation was noticeable from 0.5L to 5 L permeated volumes during compaction using all tested water qualities. Compacted membranes using MilliQ water showed lowest counts of dead/injured microorganisms throughout the compaction experiment with counts below 2×10^4 cells. cm^{-2} .

A significant increase in dead-injured cell counts was noticeable for membranes compacted with deionized and tap water only after 5L volume permeation.

3.4 Dynamic adhesion assay on compacted NF 270 membranes using different water grades.

Dynamic adhesion assays were performed on compacted membranes to establish whether permeation using different water qualities could affect the initial adhesion of *Ps. fluorescens* in terms of amount deposited on membranes and their deposition rates. Adhesion results of *Ps. fluorescens* cells conducted on compacted membranes which underwent 5 L permeation volumes of different water qualities are presented in Figure 6 and Table 3.

Different adhesion profiles were observed for *Ps. fluorescens* cells on the different compacted membranes during the 30 minutes period. Cell adhesion was highest on membranes compacted with MilliQ water after 30 minutes with 2.6×10^5 cells.cm⁻² followed by cell deposition on membranes compacted with tap water at 1.0×10^5 cells.cm⁻² (Figure 6). Cell deposition was lowest on membranes compacted with deionized water at 0.2×10^5 cells.cm⁻². The order of total cells adhered on the different surfaces after 30 min showed the following order: DI<tap<MilliQ water. The experimental data allowed maximum cell loadings on the different membranes to be deduced based on kinetic model (cf. eq.2). Membranes compacted with MilliQ water revealed highest maximum cell loadings at 2.6×10^5 cells×cm⁻², being 5 times higher than cell loadings on membranes compacted with deionized water (Table 3). No maximum could be established after 30 minutes adhesion on membranes compacted with tap water (Figure 6) since the adhesion was still in its linear phase after 30 minutes of the experiment. However, Figure 6 clearly shows that q_{max} on membranes

compacted with tap water is higher than the q_{max} value obtained for membranes compacted with deionized water. Adhesion velocity was found to be slowest on membranes compacted with deionized water at $1.06 \times 10^{-5} \text{ cm.min}^{-1}$ and tap water at $3.13 \times 10^{-5} \text{ cm.min}^{-1}$. *Ps. fluorescens* cells expressed highest adhesion velocities on membranes compacted with MilliQ water at $11.7 \times 10^{-5} \text{ cm.min}^{-1}$ (Table 3).

4 Discussion

The aim of this study was to investigate the effects of laboratory water quality during pre-compaction of nanofiltration membranes in terms of performance, surface property changes as well as its influence on standard bio-adhesion assays.

Filtration performance together with the physicochemical, physical properties and biological assessment of NF270 membrane surface were analysed at 0.5L, 2L and 5L set permeation volumes during compaction with different water sources. The dynamic bioadhesion assays were subsequently performed on the compacted NF 270 membranes using *Ps. fluorescens* cells, and experimental data was used to calculate adhesion rates as well as estimate maximum cell loadings on membranes. This allowed conclusions to be drawn about the consequential effects of laboratory water quality in membrane compaction of nanofiltration processes.

Results obtained in this study show that the water quality used during compaction of membranes, a prerequisite in most membrane research laboratories, will most certainly affect membrane surface physicochemical properties prior to performing key experiments

involving bacterial adhesion. Such changes on the membrane's surface due to membrane pre-treatment might be the basis of experimental biases. Indeed, membrane compaction is in itself a form of filtration whereby the elements found in the water will end up deposited on the membrane's surface.

Membrane performance in terms of permeate flux is directly linked to water quality. The observed higher decrease of the permeate flux with increased permeated volume of tap water compared to DI and MilliQ water was caused by a higher concentration in the feed solution of organic matter, ions and dissolved solids which, not only led to the formation of a thicker fouling layer on the membrane surface, but also led to a higher osmotic pressure difference between the feed and the permeate side. In this case, a combination of the cake build-up on the membrane surface and higher ionic concentration on the feed side can aggravate the permeate flux decline due to cake enhanced concentration polarisation (Hoek and Elimelech 2003). Moreover this fouling was also visible in the form of a coloration gradient as the volume of water permeated through the membrane increased: the degree of membrane coloration (yellow coloration) increased with increasing permeation volume and decreasing water purity. A study by Van der Bruggen and Vandecasteele (2001) showed that flux decline during nanofiltration was predominantly caused by adsorption of organic compounds in aqueous solution onto the membrane, leading to the blocking of pores.

It might be surprising that the amount of microorganisms in DI water is higher compared to tap water, as DI water is purified tap water. However, the ion exchange resin has been found to be a good place for microorganisms to adhere onto and proliferate (Flemming 1987) for several reasons: (1) the negatively charged solutes such as TOC and other nutrients such as nitrate are removed from the water by the ion exchange resin and

consumed by the microorganisms in the resin, (2) nutrients dissolved in tap water are used by the microorganisms in the ion exchange resin as a food source and (3) the resin itself is a possible food source for bacteria as it can leach solutes to the solution.

The deposition of solutes on the membrane surface will inevitably change the membrane surface properties. The observed change in surface hydrophobicity in NF270 membranes was dependent on the water used during compaction. The NF 270 membrane, known for its hydrophilic properties (Boussu et al. (2006)), became more hydrophobic following compaction with tap and deionized water respectively. In an earlier study, Her *et al.* ((2008)) demonstrated that the levels of hydrophobic and hydrophilic fractions in Natural Organic Matter (NOM) found in water that deposited onto NF membranes determined the change in surface hydrophobicity. Likewise, the observed difference in surface hydrophobicity following compaction could have been attributed to the original fraction of hydrophilic levels of NOM found in the tested water. Interestingly, membranes compacted with deionized water having a factor 6 times less total organic carbon than tap water, were found to be most hydrophobic. This may suggest that the deionized water in this study might have contained a higher fraction of hydrophobic NOM, most likely caused by leachable residuals from the ion exchange resin of the laboratory's water purifier. Surprisingly, the biological content of the deionized water was also found to be prominent. The combination of high TOC biological levels found in deionized water might be an indication of a possible polluted and contaminated ion exchange resin. Accordingly, simple conductivity measurements should not be the sole basis for verifying the purity of deionized water. Moreover, the use of sterilized deionized water would only kill the microorganisms present, but not prevent their deposition on the membrane surface after compaction (Figure 7).

488 The change in surface properties following membrane compaction was sufficient to
489 influence bacterial adhesion rates. Membranes compacted with MilliQ water attained the
490 highest bioadhesion and adhesion velocities followed by membranes compacted with tap
491 water and deionized respectively. Surprisingly, the extent of cell adhesion was not
492 proportional to hydrophobicity. Despite hydrophobicity being pinpointed as one of the
493 causes for higher adhesion onto surfaces (Lee et al. (2010), Myint et al. (2010), Subramani
494 and Hoek (2008)), it does not in itself explain the adhesion extent of the bacteria in this
495 study: the MilliQ water compacted membrane despite being more hydrophilic has a higher
496 cell adhesion than the more hydrophobic surfaces of the tap and DI water compacted
497 membranes. This indicates that surface hydrophobicity is not the sole determining factor in
498 cell adhesion in this study and factors other than surface hydrophobicity, such as surface
499 topology, could play more prominent role in bioadhesion. Membranes compacted with
500 deionized and tap water, whose surfaces were covered by a fouling layer, were showed to
501 have an unaltered surface topology compared to MilliQ water compacted membranes. The
502 surface heterogeneities found on membranes compacted with MilliQ water might explain
503 the observed higher bacterial adhesion compared to the smoother and more homogenous
504 membranes following deionized and tap water compactations. A study conducted on NF 270
505 membranes, linked bacterial adhesion to surface heterogeneities (Subramani and Hoek
506 2008). Another similar study showed that surface roughness, or more specifically surface
507 topography capable of accommodating bacterial cells, was particularly favourable for
508 bacterial adhesion compared to other types of surface (Medilanski et al. 2002). In general,
509 surface roughness can create conditions for the favourable initial adhesion of a single
510 bacterium, possibly in a topological feature and this in turn forms the seed for the
511 subsequent growth of a micro-colony. The roughness values obtained in this study were

performed under dehydrated compacted membranes, giving rise to high roughness readings and artefacts in the form of surface cracks. However, when a specific area of 20 μm by 20 μm without cracks was analysed with the profilometer software, surface roughness was still higher for the tap water compacted membrane ($425.2 \text{ nm} \pm 152.9$) compared to the roughness obtained for DI water ($164 \text{ nm} \pm 51.7$) and MilliQ water ($60.5 \text{ nm} \pm 17.2$) compacted membranes.

The presence of microorganisms on RO/NF membranes following compaction could lead to significant degrees of bias when performing adhesion and biofouling assays. This is especially important when studying biofouling using a monoculture system. The presence of viable organisms on freshly compacted membrane would most certainly lead to the development of unanticipated outcomes.

5 Conclusion

The impact of laboratory water quality was assessed following compaction of the NF membrane by analysing the membrane performance and surface characteristics, as well as the adhesion characteristics of *P. fluorescens*. Tap and DI water compaction resulted in a cake layer on the membrane surface consisting of living and dead bacteria and diatoms, organic matter, dissolved solids and other components, as these were present in the water used for compaction. There was a clear difference in the performance characteristics of the different membranes following compaction with different water types. Compacting with DI and tap water resulted in a lower permeate flux and cell adhesion rate compared to MilliQ water. In contrast, compaction with MilliQ water generated the highest fluxes through the membrane and a significantly higher initial adhesion of *P. fluorescens*. The reasons for the

different cell adhesion rates is difficult to elucidate due to the complexity of the tap and DI water. However, there seems to be a correlation with the topography of the surface: large heterogeneities on the surface seem to enhance *P. fluorescens* adhesion.

Overall, these results illustrate the importance of laboratory water quality in the compaction stage of NF/RO experiments and the consequent impact it has when undertaking bacterial adhesion studies. It needs to be noted while tap and DI water quality will vary significantly from laboratory to laboratory, these differences in quality can make it difficult to compare results of adhesion studies from different research groups. The present study identifies the need for standardized protocols for studying membrane biofouling in laboratory conditions, particularly with respect to the water quality during membrane compaction procedures and for the feed solutions in subsequent experiments.

Acknowledgments

This research was supported by the European Research Council (ERC), project 278530, funded under the EU Framework Programme 7 and also with the financial support of Science Foundation Ireland under Grant Number “SFI 11/RFP.1/ENM/3145. The authors would like to thank Dr. Dennis Dowling and the Surface Engineering research group at UCD. We thank Dr. Ian Reid of the NIMAC microscopy platform UCD. We thank Mr. Pat O'Halloran for his invaluable technical assistance, and Mr. Liam Morris for the construction of the MFS devices.

- Cyna, B., Chagneau, G., Bablon, G. and Tanghe, N. (2002) Two years of nanofiltration at the Méry554 sur-Oise plant, France. *Desalination* 147(1–3), 69-75.
- Flemming, H.C. (1997) Reverse osmosis membrane biofouling. *Experimental Thermal and Fluid Science* 14(4), 382-391.
- Ivnitsky, H., Katz, I., Minz, D., Volvovic, G., Shimoni, E., Kesselman, E., Semiat, R. and Dosoretz, C.G. (2007) Bacterial community composition and structure of biofilms developing on nanofiltration membranes applied to wastewater treatment. *Water Research* 41(17), 3924-3935.
- Flemming, H.C. (2002) Biofouling in water systems – cases, causes and countermeasures. *Applied Microbiology and Biotechnology* 59(6), 629-640.
- Houari, A., Seyer, D., Couquard, F., Kecili, K., Démocrate, C., Heim, V. and Martino, P.D. (2009) Characterization of the biofouling and cleaning efficiency of nanofiltration membranes. *Biofouling* 26(1), 15-21.
- Vrouwenvelder, H.S., van Paassen, J.A.M., Folmer, H.C., Hofman, J.A.M.H., Nederlof, M.M. and van der Kooij, D. (1998) Biofouling of membranes for drinking water production. *Desalination* 118(1–3), 157-166.
- Vrouwenvelder, J.S., Manolarakis, S.A., van der Hoek, J.P., van Paassen, J.A.M., van der Meer, W.G.J., van Agtmaal, J.M.C., Prummel, H.D.M., Kruithof, J.C. and van Loosdrecht, M.C.M. (2008) Quantitative biofouling diagnosis in full scale nanofiltration and reverse osmosis installations. *Water Research* 42(19), 4856-4868.
- Khan, M.T., Manes, C.-L.d.O., Aubry, C. and Croué, J.-P. (2013) Source water quality shaping different fouling scenarios in a full-scale desalination plant at the Red Sea. *Water Research* 47(2), 558-568.
- Flemming, H.C., Schaule, G., Griebel, T., Schmitt, J. and Tamachkierowa, A. (1997) Biofouling—the Achilles heel of membrane processes. *Desalination* 113(2–3), 215-225.
- Hijnen, W.A.M., Castillo, C., Brouwer-Hanzens, A.H., Harmsen, D.J.H., Cornelissen, E.R. and van der Kooij, D. (2012) Quantitative assessment of the efficacy of spiral-wound membrane cleaning procedures to remove biofilms. *Water Research* 46(19), 6369-6381.
- Vrouwenvelder, J.S., Hinrichs, C., Van der Meer, W.G.J., Van Loosdrecht, M.C.M. and Kruithof, J.C. (2009a) Pressure drop increase by biofilm accumulation in spiral wound RO and NF membrane systems: role of substrate concentration, flow velocity, substrate load and flow direction. *Biofouling* 25(6), 543-555.
- Hijnen, W.A.M., Biraud, D., Cornelissen, E.R. and van der Kooij, D. (2009) Threshold Concentration of Easily Assimilable Organic Carbon in Feedwater for Biofouling of Spiral-Wound Membranes. *Environmental Science & Technology* 43(13), 4890-4895.
- Ivnitsky, H., Katz, I., Minz, D., Shimoni, E., Chen, Y., Tarchitzky, J., Semiat, R. and Dosoretz, C.G. (2005) Characterization of membrane biofouling in nanofiltration processes of wastewater treatment. *Desalination* 185(1–3), 255-268.
- Huertas, E., Herzberg, M., Oron, G. and Elimelech, M. (2008) Influence of biofouling on boron removal by nanofiltration and reverse osmosis membranes. *Journal of Membrane Science* 318(1–2), 264-270.
- Herzberg, M. and Elimelech, M. (2007) Biofouling of reverse osmosis membranes: Role of biofilm593 enhanced osmotic pressure. *Journal of Membrane Science* 295(1–2), 11-20.
- Chong, T.H., Wong, F.S. and Fane, A.G. (2008) The effect of imposed flux on biofouling in reverse osmosis: Role of concentration polarisation and biofilm enhanced osmotic pressure phenomena. *Journal of Membrane Science* 325(2), 840-850.
- Vrouwenvelder, J.S., Graf von der Schulenburg, D.A., Kruithof, J. 597 C., Johns, M.L. and van Loosdrecht,

607 M.C.M. (2009b) Biofouling of spiral-wound nanofiltration and reverse osmosis membranes: A feed
 608 spacer problem. *Water Research* 43(3), 583-594.
 609 Ridgway, H.F., Rigby, M.G. and Argo, D.G. (1985) Bacterial Adhesion and Fouling of Reverse Osmosis
 610 Membranes. *Journal of American Water Works Association* 77(7), 97-106.
 611 Subramani, A. and Hoek, E.M.V. (2008) Direct observation of initial microbial deposition onto
 612 reverse
 613 osmosis and nanofiltration membranes. *Journal of Membrane Science* 319(1–2), 111-125.
 614 Myint, A.A., Lee, W., Mun, S., Ahn, C.H., Lee, S. and Yoon, J. (2010) Influence of membrane surface
 615 properties on the behavior of initial bacterial adhesion and biofilm development onto nanofiltration
 616 membranes. *Biofouling* 26(3), 313-321.
 617 Khan, M.M.T., Stewart, P.S., Moll, D.J., Mickols, W.E., Nelson, S.E. and Camper, A.K. (2011)
 618 Characterization and effect of biofouling on polyamide reverse osmosis and nanofiltration
 619 membrane surfaces. *Biofouling* 27(2), 173-183.
 620 Subramani, A., Huang, X. and Hoek, E.M.V. (2009) Direct observation of bacterial deposition onto
 621 clean and organic-fouled polyamide membranes. *Journal of Colloid and Interface Science* 336(1), 13-
 622 20.
 623 Baek, Y., Yu, J., Kim, S.-H., Lee, S. and Yoon, J. (2011) Effect of surface properties of reverse osmosis
 624 membranes on biofouling occurrence under filtration conditions. *Journal of Membrane Science*
 625 382(1–2), 91-99.
 626 Fonseca, A.C., Summers, R.S., Greenberg, A.R. and Hernandez, M.T. (2007) Extra-Cellular
 627 Polysaccharides, Soluble Microbial Products, and Natural Organic Matter Impact on Nanofiltration
 628 Membranes Flux Decline. *Environmental Science & Technology* 41(7), 2491-2497.
 629 Miller, D.J., Araújo, P.A., Correia, P.B., Ramsey, M.M., Kruithof, J.C., van Loosdrecht, M.C.M.,
 630 Freeman, B.D., Paul, D.R., Whiteley, M. and Vrouwenvelder, J.S. (2012) Short-term adhesion and
 631 long-term biofouling testing of polydopamine and poly(ethylene glycol) surface modifications of
 632 membranes and feed spacers for biofouling control. *Water Research* 46(12), 3737-3753.
 633 Bernstein, R., Belfer, S. and Freger, V. (2011) Bacterial Attachment to RO Membranes Surface-
 634 Modified by Concentration-Polarization-Enhanced Graft Polymerization. *Environmental Science &*
 635 *Technology* 45(14), 5973-5980.
 636 Suwarno, S.R., Chen, X., Chong, T.H., Puspitasari, V.L., McDougald, D., Cohen, Y., Rice, S.A. and Fane,
 637 A.G. (2012) The impact of flux and spacers on biofilm development on reverse osmosis membranes.
 638 *Journal of Membrane Science* 405–406(0), 219-232.
 639 Vrouwenvelder, J.S., van Paassen, J.A.M., van Agtmaal, J.M.C., van Loosdrecht, M.C.M. and Kruithof,
 640 J.C. (2009c) A critical flux to avoid biofouling of spiral wound nanofiltration and reverse osmosis
 641 membranes: Fact or fiction? *Journal of Membrane Science* 326(1), 36-44.
 642 Vrouwenvelder, J.S., Bakker, S.M., Wessels, L.P. and van Paassen, J.A.M. (2007) The Membrane
 643 Fouling Simulator as a new tool for biofouling control of spiral-wound membranes. *Desalination*
 644 204(1–3), 170-174.
 645 Botton, S., Verliefde, A.R.D., Quach, N.T. and Cornelissen, E.R. (2012) Influence of biofouling on
 646 pharmaceuticals rejection in NF membrane filtration. *Water Research* (0).
 647 Khan, M.M.T., Stewart, P.S., Moll, D.J., Mickols, W.E., Burr, M.D., Nelson, S.E. and Camper, A.K.
 648 (2010) Assessing biofouling on polyamide reverse osmosis (RO) membrane surfaces in a laboratory
 649 system. *Journal of Membrane Science* 349(1–2), 429-437.
 650 Lee, W., Ahn, C.H., Hong, S., Kim, S., Lee, S., Baek, Y. and Yoon, J. (2010) Evaluation of surface
 651 properties of reverse osmosis membranes on the initial biofouling stages under no filtration
 652 condition. *Journal of Membrane Science* 351(1–2), 112-122.
 653 Chong, T.H., Wong, F.S. and Fane, A.G. (2007) Enhanced concentration polarization by unstirred
 654 fouling layers in reverse osmosis: Detection by sodium chloride tracer response technique. *Journal*
 655 *of Membrane Science* 287(2), 198-210.
 656 Pang, C.M., Hong, P., Guo, H. and Liu, W.-T. (2005) Biofilm 646 Formation Characteristics of Bacterial
 657 Isolates Retrieved from a Reverse Osmosis Membrane. *Environmental Science & Technology* 39(19),

658 7541-7550.

659 Gibbs, R.A., Scutt, J.E. and Croll, B.T. (1993) Assimilable Organic Carbon Concentrations and Bacterial

660 Numbers in a Water Distribution System. *Water Science & Technology* 27(3-4), 159-166.

661 Vrouwenvelder, J.S., van Paassen, J.A.M., Wessels, L.P., van Dam, A.F. and Bakker, S.M. (2006) The

662 Membrane Fouling Simulator: A practical tool for fouling prediction and control. *Journal of*

663 *Membrane Science* 281(1-2), 316-324.

664 Hoek, E.M.V. and Elimelech, M. (2003) Cake-Enhanced Concentration Polarization: A New Fouling

665 Mechanism for Salt-Rejecting Membranes. *Environmental Science & Technology* 37(24), 5581-5588.

666 Van der Bruggen, B. and Vandecasteele, C. (2001) Flux Decline during Nanofiltration of Organic

667 Components in Aqueous Solution. *Environmental Science & Technology* 35(17), 3535-3540.

668 Flemming, H.-C. (1987) Microbial growth on ion exchangers. *Water Research* 21(7), 745-756.

669 Boussu, K., Zhang, Y., Cocquyt, J., Van der Meeren, P., Volodin, A., Van Haesendonck, C., Martens,

670 J.A. and Van der Bruggen, B. (2006) Characterization of polymeric nanofiltration membranes for

671 systematic analysis of membrane performance. *Journal of Membrane Science* 278(1-2), 418-427.

672 Her, N., Amy, G., Chung, J., Yoon, J. and Yoon, Y. (2008) Characterizing dissolved organic matter and

673 evaluating associated nanofiltration membrane fouling. *Chemosphere* 70(3), 495-502.

674 Medilanski, E., Kaufmann, K., Wick, L.Y., Wanner, O. and Harms, H. (2002) Influence of the Surface

675 Topography of Stainless Steel on Bacterial Adhesion. *Biofouling* 18(3), 193-203.

676

677

678

679

680 **List of Tables**

681 Table 1 Chemical and biological characterisation of the different water qualities used during
682 the membrane compaction study.

683

684 Table 2 NF 270 membrane surface properties after compaction with different water sources
685 at different permeate volumes.

686

687 Table 3: Estimated maximum cell loading and adhesion velocity values of *Ps. fluorescens*
688 cells on compacted NF270 membranes with different water qualities. Error is represented as
689 standard error.

690

691

List of Figures

Figure 1 MFS Cross-Flow system.

Figure 2 Flux decline of the NF 270 membrane during compaction with different water sources (0.5, 2 and 5 L of source water filtered, 0.66 L.min⁻¹ in each MFS, 15 bar and 21°C). Each experiment was repeated twice. The error bar represents the variability of the flux obtained for all the membranes used in duplicate exposed to that particular permeate volume (0.5, 2 and 5 L).

Figure 3 Height topography of a compacted membrane with MilliQ (A), DI (B) and tap water(C) were obtained by optical profilometry (223×293 µm). The 2D images associated to each profile are shown, all X and Y axes are in microns.

Figure 4 Scanning electron micrographs of non-compacted NF 270 membranes (A) and compacted NF270 membranes after 5L permeated volumes of Milli Q water (B), deionized water (C), and tap water (D) at 0.66 L•min⁻¹, 15 bar and 21°C .

Figure 5 Number of accumulated microorganisms on NF270 membranes following compaction with increasing permeated volumes of different water qualities. Error bars represent standard error.

713 Figure 6 Dynamic adhesion of *Ps. fluorescens* cells on compacted NF-270 membranes after
714 5L permeated volumes of different water qualities.

715

716 Figure 7 Fluorescence micrographs showing membrane samples following membrane
717 compaction with autoclaved DI water at 15 bar stained with (A) Syto 9 and (B) Propidium
718 Iodide and membrane compaction with non-autoclaved DI water at 15 bar stained with (C)
719 Syto 9 and (D) Propidium Iodide

720

721 Table 1

Water Quality	MilliQ Water	Deionized Water	Tap Water
Total Solids (mg•L ⁻¹)	ND*	ND*	109.17 ± 5.2
pH	6.01 ± 0.11	6.31 ± 0.29	7.44 ± 0.07
TOC (mg•C•L ⁻¹)	0.04 ± 0.04	1.6 ± 0.7	9.6 ± 0.8
Conductivity (μS•cm ⁻¹)	0.4 ± 0.1	4 ± 2	168 ± 7
Culturable counts (Cells•mL ⁻¹)	ND*	239	1.4
Total cell counts (10 ³ Cells•mL ⁻¹)	1 ± 1	1472 ± 421	123 ± 47
Total dead/injured counts (10 ³ Cells•mL ⁻¹)	3 ± 2	2020 ± 482	82 ± 44

722 *ND: not detected

723

724

725

726

1

2 Table 2

3

	Permeated volume	Compacted NF 270 membranes								
		MilliQ water			Deionized water			Tap water		
		0.5L	2L	5L	0.5L	2L	5L	0.5L	2L	5L
Contact angle	θ_{water}	40.5 ± 1.11	45.5 ± 0.89	49.7 ± 0.58	55.7 ± 0.34	64.3 ± 0.45	68.9 ± 0.63	45.8 ± 0.9	53.4 ± 0.6	56.0 ± 3.9
	$\theta_{\text{diiodomethane}}$	36.6 ± 0.41	36.9 ± 0.88	34.4 ± 0.67	45.3 ± 0.56	46.8 ± 0.88	44.6 ± 0.97	38.6 ± 0.7	36.4 ± 1.6	28.7 ± 6.7
	$\theta_{\text{ethylene glycol}}$	28.9 ± 0.98	25.8 ± 0.73	26.6 ± 0.42	34.6 ± 0.64	41.5 ± 0.81	47.8 ± 0.59	32.9 ± 0.9	36.7 ± 0.7	40.6 ± 5.6
Surface tension (mJ•m ⁻²)	γ^{LW}	41.4 ± 0.18	41.3 ± 0.41	42.3 ± 0.33	36.9 ± 0.31	35.7 ± 0.51	37.0 ± 0.56	40.3 ± 0.4	41.9 ± 0.7	45.5 ± 0.5
	γ^-	49.1 ± 1.83	44.8 ± 1.4	33.7 ± 0.99	28.5 ± 0.55	19.9 ± 0.85	17.8 ± 1.24	44.9 ± 1.4	35.5 ± 1.2	33.4 ± 1.2
	γ^+	0.1 ± 0.04	0.04 ± 0.01	0.03 ± 0.01	0.1 ± 0.02	0.2 ± 0.04	0.08 ± 0.02	0.15 ± 0.05	0.19 ± 0.04	0.55 ± 0.1
	γ^{AB}	4.06 ± 0.6	2.22 ± 0.4	1.86 ± 0.32	3.9 ± 0.4	4.9 ± 0.6	2.77 ± 0.4	3.94 ± 0.73	4.80 ± 0.8	9.1 ± 0.9
	γ^{S}	53.2 ± 2.3	47.0 ± 1.65	35.6 ± 1.03	32.5 ± 0.4	24.8 ± 0.7	20.6 ± 1.32	48.9 ± 1.9	40.3 ± 1.8	42.6 ± 2.04
Surface roughness (RMS) (nm)	200 µm x 200 µm surface area *	468 ± 142	417 ± 121	511 ± 143	452 ± 177	592 ± 144	562 ± 123	521 ± 160	695 ± 251	1166 ± 147

4

5 * Roughness deduced from surface profilometry.

6

7

1

2 **Table 3**

	Compacted NF 270 membranes			3
	MilliQ water	Deionized water	Tap water	4
Estimated maximum cell loading q_{\max} (10^4 Cells \cdot cm $^{-2}$)	26 ± 2.5	5.2 ± 1.3	ND	5
Adhesion velocity k_d (10^{-5} cm \cdot min $^{-1}$)	11.7 ± 2.4	1.06 ± 0.09	3.13 ± 0.3	6 7

8

9 *ND: not determined.

10

11

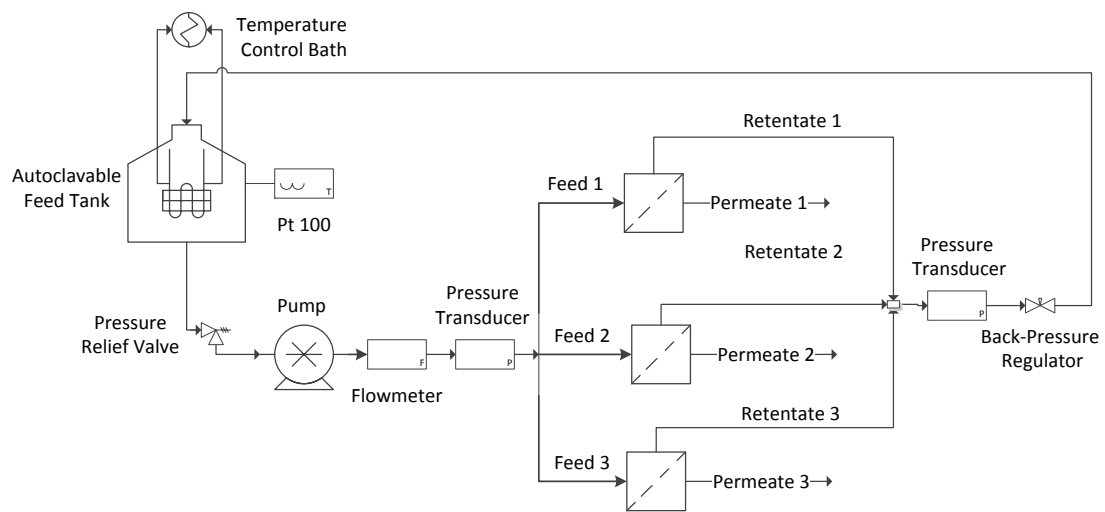
12

13

14

1 Figure 1

2



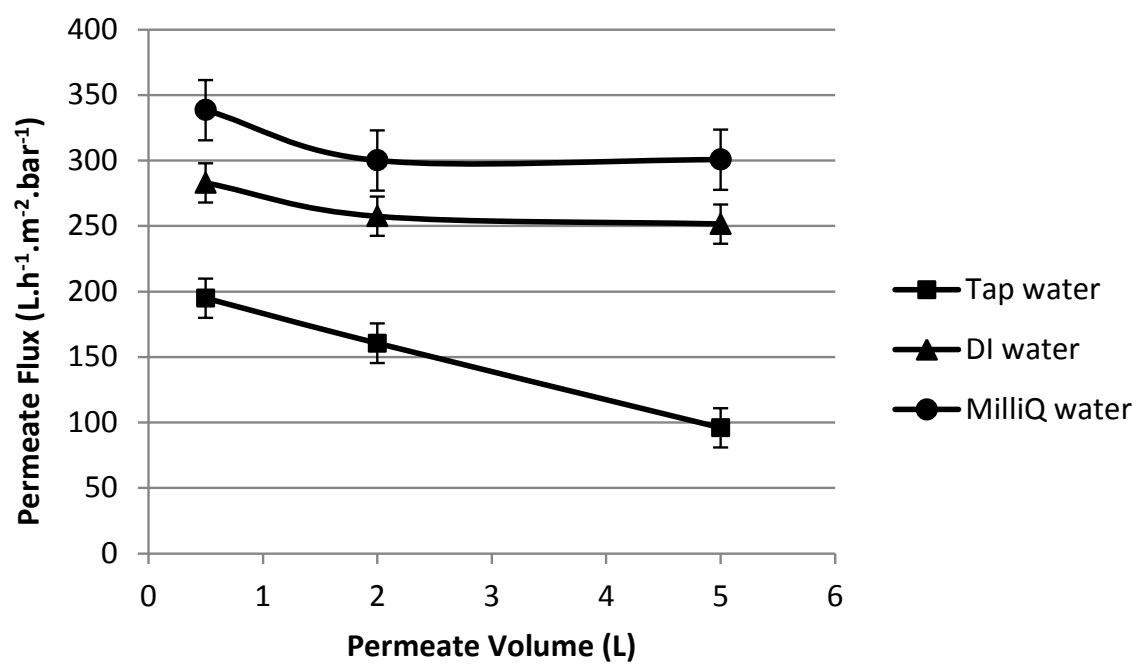
3

4

1

2

3 Figure 2



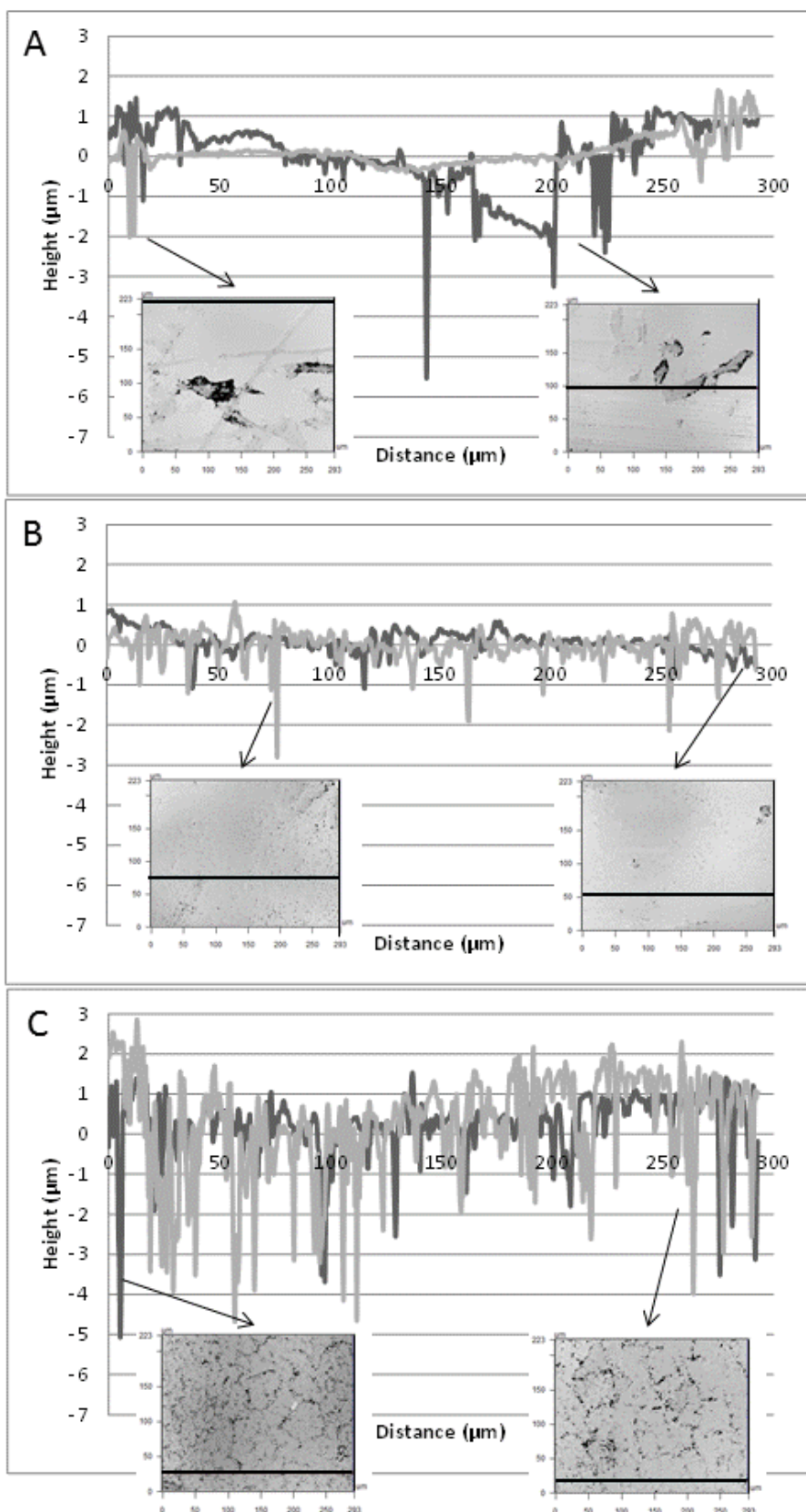
4

5

6

1

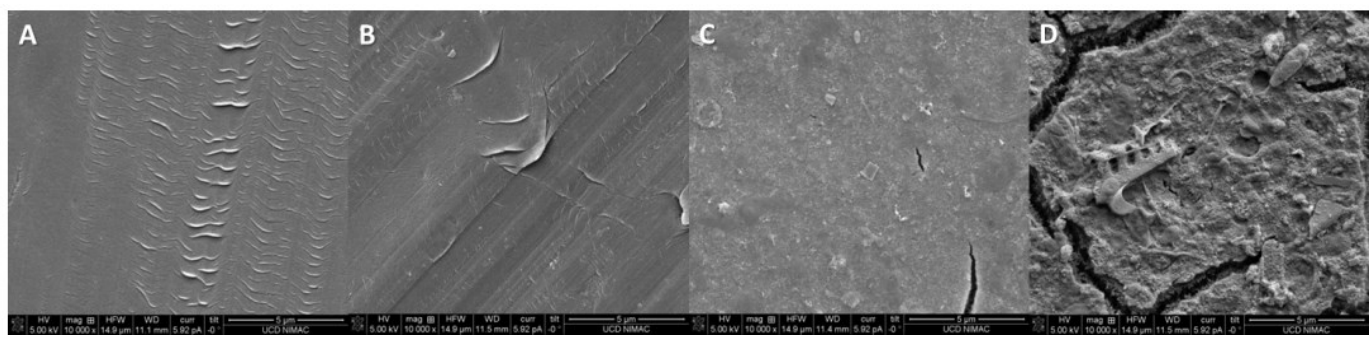
2 Figure 3



3

1

2 **Figure 4**



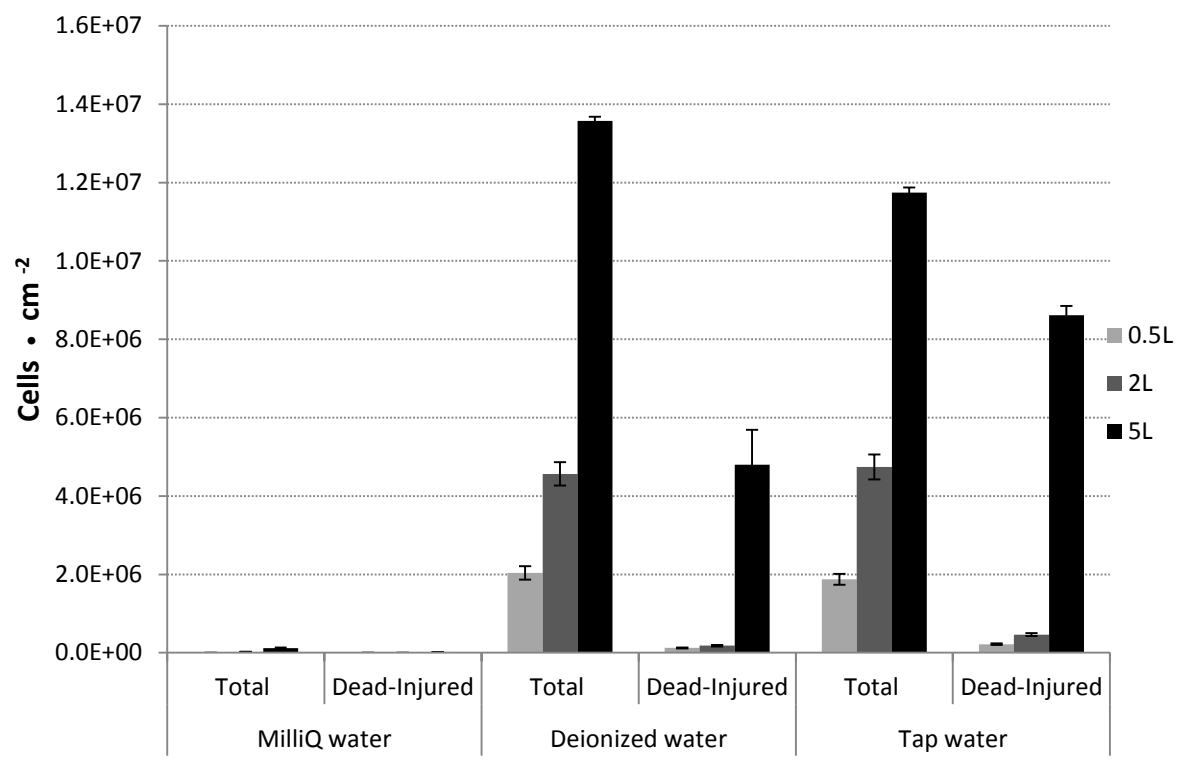
3

4

5

1

2 **Figure 5**



3

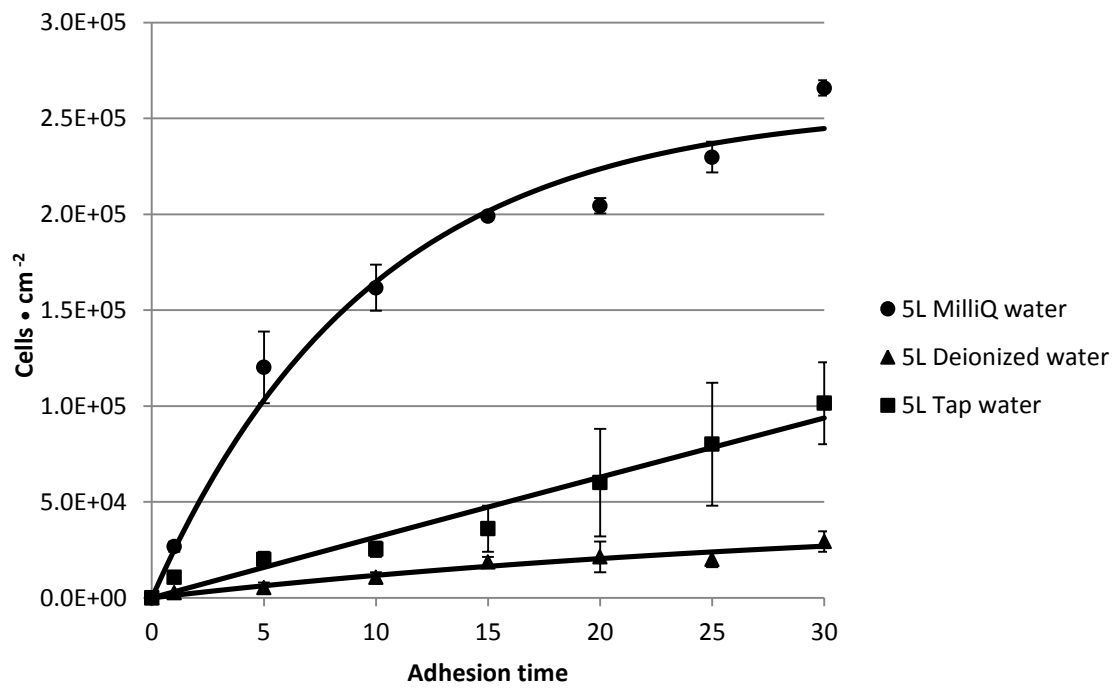
4

5

1

2

3 Figure 6



4

5

6

1 Figure 7

